Autologous minced muscle grafts: a tissue engineering therapy for the volumetric loss of skeletal muscle

B. T. Corona, K. Garg, C. L. Ward, J. S. McDaniel, T. J. Walters, and C. R. Rathbone

Extremity Trauma and Regenerative Medicine Research Program, United States Army Institute of Surgical Research, Fort Sam Houston, Texas

Corona BT, Garg K, Ward CL, McDaniel JS, Walters TJ, Rathbone CR. Autologous minced muscle grafts: a tissue engineering therapy for the volumetric loss of skeletal muscle. *Am J Physiol Cell Physiol* 305: C761–C775, 2013. First published July 24, 2013; doi:10.1152/ajpcell.00189.2013.—Volumetric muscle loss (VML) results in a large void deficient in the requisite materials for regeneration for which there is no definitive clinical standard of care. Autologous minced muscle grafts (MG), which contain the essential components for muscle regeneration, may embody an ideal tissue engineering therapy for VML. The purpose of this study was to determine if orthotopic transplantation of MG acutely after VML in the tibialis anterior muscle of male Lewis rats promotes functional tissue regeneration. Herein we report that over the first 16 wk postinjury, MG transplantation *1*) promotes remarkable regeneration of innervated muscle fibers within the defect area (i.e., de novo muscle fiber regeneration); *2*) reduced evidence of chronic injury in the remaining muscle mass compared with nonrepaired muscles following VML (i.e., transplantation attenuated chronically upregulated transforming growth factor-β_1 gene expression and the presence of centrally located nuclei in 30% of fibers observed in nonrepaired muscles); and *3*) significantly improves net torque production (i.e., ∼55% of the functional deficit in nonrepaired muscles was restored). Additionally, voluntary wheel running was shown to reduce the heightened accumulation of extracellular matrix deposition observed within the regenerated tissue of MG-repaired sedentary rats 8 wk postinjury (collagen 1% area: sedentary vs. runner, ∼41 vs. 30%), which may have been the result of an augmented inflammatory response [i.e., M_1 (CCR7) and M_2 (CD163) macrophage expression was significantly greater in runner than sedentary MG-repaired muscles 2 wk postinjury]. These findings support further exploration of autologous minced MGs for the treatment of VML.

minced muscle graft; volumetric muscle loss; skeletal muscle injury and damage; tissue engineering; tissue regeneration

VOLUMETRIC MUSCLE LOSS (VML), defined as "the traumatic or surgical loss of skeletal muscle with resultant functional impairment" (22), is common in civilian and military populations following penetrating extremity trauma, crush injuries, and compartment syndrome and is often a comorbidity to open bone fracture (9, 18, 21, 32, 42). In both preclinical animal models and in humans, VML results in an irrecoverable loss of functional muscle tissue (16, 36, 69, 71), and muscle synergist compensatory hypertrophy is incapable of restoring function to the muscle unit (36, 69, 71). There is no clinical standard of care for VML, and treatment options are limited. In severe cases, functional muscle transfers have been performed successfully (32), although considerable surgical experience is required to perform these procedures. Additionally, in military populations physical therapy with the aid of IDEO bracing, a polycarbonate brace that allows for limb loading, has resulted in improved performance on physical assessment batteries (43). However, it remains unclear as to whether or not the remaining muscle mass after VML maintains the capacity for plasticity in response to physical therapy. Overall, the etiology of VML is not understood.

Skeletal muscle regeneration requires a complex interaction among numerous cell types and tissues. Mammalian muscle can self-repair, regenerate, and remodel if the basal lamina remains relatively intact (10, 35), satellite cells are activated (30, 45), an appropriate inflammatory response ensues (60, 67), and supporting vascular (38), neural (20), and cellular (e.g., fibroblasts; Ref. 40) elements are present. This is apparent in a variety of animal injury models, such as toxin (44), freeze (67), eccentric contraction (34), laceration (31), and ischemia-reperfusion injury (17), in which severely damaged tissue undergoes significant, if not complete, regeneration. Conversely, with VML there is a void in the tissue wherein basal lamina and other supporting elements are unable to serve as a foundation for myofiber regeneration. As a result, regeneration is aberrant with the remaining muscle mass undergoing an atrophic remodeling, marked by fibrosis and chronic muscle fiber damage (16, 69).

Over the past decade there has been an emphasis on developing tissue engineering therapies for the repair of VML. A paradigm has been adopted in which isolated components of the basic elements for regeneration are transplanted to the defect site. For instance, biological decellularized extracellular matrix materials (ECM) have been transplanted to the site of VML or VML-like injuries (63, 65). It is thought that the transplanted ECMs promote a targeted immune response, mediating constructive remodeling within the defect (64). This process relies on the migration of myogenic cells from the host, which may be hindered in many conceivable ways (e.g., fibrous tissue formation), and therefore appears to require an extended postsurgical time to observe significant skeletal muscle fiber regeneration (63), if at all (14, 62). In an attempt to hasten and ultimately improve regenerative outcomes, ECMs have been supplemented with stem or progenitor cells (e.g., Refs. 14, 37). For example, mesenchymal stem cells delivered to ECMs at the site of injury have been shown to enhance muscle tissue regeneration after VML (37) and laceration injury (41), although this is not always the case (16).

Since tissue engineering strategies aim to recapitulate normal regenerative processes, it seems pertinent to regard the contribution of satellite cells given their well-documented role throughout all phases of muscle regeneration (30, 50). Recently, several reports have demonstrated the usefulness of

Address for reprint requests and other correspondence: B. T. Corona, Extremity Trauma and Regenerative Medicine, US Army Institute of Surgical Research, 3698 Chambers Pass, Fort Sam Houston, TX 78234 (e-mail: benjamin.t.corona.vol@mail.mil).

Report Documentation Page		*Form Approved* *OMB No. 0704-0188*

Public reporting burden for the collection of information is estimated to average 1 hour per response, including the time for reviewing instructions, searching existing data sources, gathering and maintaining the data needed, and completing and reviewing the collection of information. Send comments regarding this burden estimate or any other aspect of this collection of information, including suggestions for reducing this burden, to Washington Headquarters Services, Directorate for Information Operations and Reports, 1215 Jefferson Davis Highway, Suite 1204, Arlington VA 22202-4302. Respondents should be aware that notwithstanding any other provision of law, no person shall be subject to a penalty for failing to comply with a collection of information if it does not display a currently valid OMB control number.

1. REPORT DATE **01 OCT 2013**	2. REPORT TYPE **N/A**	3. DATES COVERED **-**

4. TITLE AND SUBTITLE	5a. CONTRACT NUMBER
Autologous minced muscle grafts: A tissue engineering therapy for the volumetric loss of skeletal muscle	5b. GRANT NUMBER
	5c. PROGRAM ELEMENT NUMBER
6. AUTHOR(S)	5d. PROJECT NUMBER
Corona B. T., Garg K., Ward C. L., McDaniel J. S., Walters T. J., Rathbone C. R.,	5e. TASK NUMBER
	5f. WORK UNIT NUMBER

7. PERFORMING ORGANIZATION NAME(S) AND ADDRESS(ES) **United States Army Institute of Surgical Research, JBSA Fort Sam Houston, TX**	8. PERFORMING ORGANIZATION REPORT NUMBER

9. SPONSORING/MONITORING AGENCY NAME(S) AND ADDRESS(ES)	10. SPONSOR/MONITOR'S ACRONYM(S)
	11. SPONSOR/MONITOR'S REPORT NUMBER(S)

12. DISTRIBUTION/AVAILABILITY STATEMENT
Approved for public release, distribution unlimited

13. SUPPLEMENTARY NOTES

14. ABSTRACT

15. SUBJECT TERMS

16. SECURITY CLASSIFICATION OF:			17. LIMITATION OF ABSTRACT	18. NUMBER OF PAGES	19a. NAME OF RESPONSIBLE PERSON
a. REPORT **unclassified**	b. ABSTRACT **unclassified**	c. THIS PAGE **unclassified**	**UU**	**15**	

Standard Form 298 (Rev. 8-98)
Prescribed by ANSI Std Z39-18

single muscle fibers for the delivery of satellite cells (13, 23, 47, 57). Importantly, this technique overcomes the initial death that normally results when satellite cells are delivered as isolated cell populations (13). Despite the promise single fiber transplants hold, the need for regulatory approval and the need for expertise for the technique are limiting factors for clinical translation. Conversely, the transfer of minced muscle grafts, which are essentially bundles of single fibers, may be a technically less challenging procedure with direct translational impact (5). Further, while the transfer of single muscle fibers offers the benefit of delivering satellite cells, transplantation of minced muscle grafts delivers other cell types and a native ECM that are important to the regenerative process. The regenerative capacity of minced muscle grafts has been known for decades described extensively in the seminal articles of Studitsky (55) and Carlson (11); however, this relatively simple technique has been overlooked in the pursuit of more complex tissue engineering strategies. The purpose of this article was to determine if minced autologous grafts provide a suitable foundation for therapies of VML injury.

METHODS

Experimental Design

Male Lewis rats with VML either received no repair or were repaired with autologous minced muscle grafts. In an initial study, single housed rats with normal cage activity (sedentary; Ref. 6) from each treatment group were allotted to one of three time points postinjury: 2, 8, or 16 wk. At these times, tissue was collected for histological and molecular analyses. At 8 and 16 wk only, rats underwent in vivo mechanical functional testing of the anterior crural muscles before tissue harvest. Upon finding that the minced graft transplantation promoted de novo muscle fiber regeneration and partially restored the functional capacity of the injured muscle, a second study was performed to determine if increased activity during an 8-wk postsurgical period improved tissue regeneration. In this study, minced graft-repaired rats were given access to running wheels in their cages beginning at 1 wk postinjury and until 2 or 8 wk postinjury, at which time muscle mechanical testing (8 wk only) and tissue harvest occurred.

Animals

This work has been conducted in compliance with the Animal Welfare Act and the Implementing Animal Welfare Regulations and in accordance with the principles of the *Guide for the Care and Use of Laboratory Animals*. All animal procedures were approved by the United States Army Institute of Surgical Research Institutional Animal Care and Use Committee. Adult male Lewis rats (Harlan Laboratories, Indianapolis, IN) were housed in a vivarium accredited by the Association for the Assessment and Accreditation of Laboratory Animal Care International.

Cell Proliferation and Immunocytochemistry

Tibialis anterior (TA) muscle tissue was minced to ~1-mm³ pieces as described below, and fractions were placed in wells of a 48-well tissue culture treated plate coated with collagen [Rat Tail Collagen I (BD Biosciences) at 25 μg/cm² in 0.02 M acetic acid]. Autograft tissue was cultured in growth medium (DMEM/F-12 supplemented with 20% FBS containing 1% penicillin/streptomycin) for up to 14 days in a humidified incubator at 37°C (5% CO_2). Media were changed every 3–4 days. On *days 1, 5, 7, 10*, and *14* (*n* = 6 wells/time point), plates were washed with PBS and stored at −80°C. The CyQUANT cell proliferation assay kit (Life Technologies, Grand Island, NY) was used to measure nucleic acid content over time as an

index of cell proliferation. Briefly, the plates containing the cells were thawed, incubated with the fluorescent dye and lysis buffer from the CyQUANT kit, and read on a SpectraMax M2 plate reader (Molecular Devices, Sunnyvale, CA) with excitation at 480 nm and emission at 520 nm. DNA content was determined by correlating fluorescence measurements to a standard curve prepared using DNA diluted in the CyQUANT fluorescent dye and lysis buffer. For myogenic cell characterization, desmin immunostaining [1° Ab, desmin (Sigma); 2° Ab, Alexa Fluor 594 (Invitrogen)] was performed using standard procedures (14).

Scanning Electron Microscopy

After being minced, autograft tissue was placed in a well plate and fixed with 2.5% phosphate-buffered glutaraldehyde (0.1 Ml pH 7.2–7.4) overnight at 4°C. The tissue was then washed with PBS and dehydrated through a series of alcohol concentrations (50–100%) before air drying. The tissue was mounted to a specimen stub using double-sided carbon tape. Samples were sputter-coated with gold (108 Auto Sputter Coater; TedPella, Redding, CA) and then visualized using a Carl Zeiss VP-40 field emission scanning electron microscope (Oberkochen, Germany) operated at a scanning voltage of 2 kV.

Surgical Creation and Treatment of VML Injury

The surgical procedure for creating VML in the rat TA muscle was performed as described previously (16, 71). With the use of aseptic technique, a surgical defect of ~10 × 7 × 3 mm (length × width × depth) was created in the middle third of the TA muscle in left leg using a scalpel. The excised defect weight approximated ~20% of the estimated TA muscle weight using a regression equation based on the rat's body weight at the time of surgery, as reported previously (71). Defect weights for each experimental group are listed in RESULTS (see Table 2). As per experimental condition, TA muscles were repaired with autologous minced muscle grafts, which were created using the piece of TA muscle excised for the VML defect and mincing it using Vanna scissors into ~1-mm³ fragments. The minced tissue was then placed orthotopically into the fresh wound bed within ~10 min and held in place by the fascia that was closed using Vicryl suture. Rats were administered buprenorphine-HCl, 1.0 mg/kg sq 30 min before surgery and at 12 and 24 h postoperatively.

A subset of rats repaired with minced grafts were housed with unrestricted access to a running wheel (model 80859; Lafayette Instruments). Access was given starting 1 wk after VML injury and was continued for 1 or 7 wk (i.e., 2 or 8 wk postinjury). Running distance was monitored constantly and recorded on a PC using the hardware and software provided with the system, and the total daily distance run by each rat was determined.

In Vivo Anterior Crural Muscle Functional Testing

Anterior crural muscle in vivo mechanical properties were measured in anesthetized rats (isoflurane 1.5–2.0%) in both legs as previously described (16, 71). Core body temperature was monitored and maintained at ~36–37°C. A nerve cuff with multistranded stainless steel (632; Cooner Wire) wire electrodes was implanted in each leg around the peroneal nerve. Legs were tested separately and in a randomized order. The foot was strapped to a footplate using silk surgical tape attached to a dual-mode muscle lever system (model 305b; Aurora Scientific). The knee was secured on either side using a custom-made mounting system, and the knee and ankle were positioned at right angles. Optimal voltage (2–5 V) was set with a series of tetanic contractions (5–10 contractions; 150 Hz, 0.1-ms pulse width, 400-ms train). Maximal isometric torque of the anterior crural muscle unit [TA, extensor digitorum longus (EDL), and extensor hallucis longus (EHL) muscles] was derived from this testing. Then, a skin incision was made at the anterolateral aspect of the ankle and the distal EDL muscle tendon, and the EHL muscle was isolated and

severed above the retinaculum. The TA muscle and tendon, as well as the retinaculum, were undisturbed. Four to five tetani were performed with a 1-min rest interval to allow for torque stabilization. Preliminary testing indicated that the contribution of the tenotomized EDL muscle was negligible in this testing system (e.g., TA muscle torque with EDL distally tenotomized vs. EDL ablation, 23.1 ± 0.8 vs. 22.4 ± 0.4 N/mm; $n = 3$; $P = 0.171$). This is likely because the released EDL muscle was in an extremely shortened position and therefore produced little force upon stimulation (25). TA muscle isometric torque as function of stimulation frequency (10–200 Hz) was assessed with a 1-min rest interval (0.1-ms pulse width, 400-ms train).

Following the isometric assessment, a subset of rats ($n = 4$ per group) at 16 wk postinjury underwent TA muscle in vivo isokinetic tetanic torque testing as a function of velocity (-400–$2,000°/s$; 150 Hz). Shortening contractions (positive velocities) were performed before lengthening contractions (negative velocities) to avoid injury to the muscle. For shortening contractions, the foot started at 90° and was passively plantarflexed 19° and then the foot was dorsiflexed 38° while the muscle was stimulated (150 Hz, 0.1-ms pulse width). The train duration of the shortening contractions ranged from 19 to 380 ms for the fastest to slowest contractions, respectively. For lengthening contractions (starting at 90°), the foot was passively dorsiflexed 19°. In the dorsiflexed position, the anterior crural muscles were stimulated for 120 ms isometrically and then, while still active, plantarflexed 38°. Peak torque, work, and average power were calculated from the isokinetic contractions.

In Vivo Intramuscular Glycogen Depletion and Analysis

For a subset of rats at 8 wk postinjury, the common peroneal nerved was stimulated to deplete intramuscular glycogen within the TA muscle fibers applying the principles described by Armstrong et al. (2). This methodology was used to determine if minced graft-associated regenerated muscle fibers were innervated, as only innervated muscle fibers will become glycogen depleted in response to continuous neural stimulation (8). Four contractile fatigue bouts were performed. *Bouts 1* and *2* consisted of 100 contractions with a 1-s rest between. *Bouts 3* and *4* consisted of 150 contractions with a 0.5-s rest between contractions. A 1-min rest was given between bouts. All contractions were isometric with the following neural stimulation parameters: 100 Hz, 0.1-ms pulse width, 200-ms train. Muscles were harvested immediately following the *bout 4* and frozen for histology. TA muscles repaired with minced grafts that underwent the stimulation protocol ($n = 3$) or did not ($n = 3$) were sectioned (8 µm) and stained for glycogen (periodic acid-Schiff). Per muscle, 3–10 nonoverlapping ×20 images from the remaining muscle mass and defect area were captured for analysis. Grayscale images were thresholded to remove background from "nontissue" areas within the image, and then the mean pixel intensity was measured using ImageJ (National Institutes of Health). For reporting, the mean pixel intensity was transformed: glycogen content = 1/mean pixel intensity × 1,000.

Histological and Immunohistochemistry Analysis

TA muscles were embedded in a talcum-based gel and frozen in 2-methylbutane (Fisher Scientific) super-cooled in liquid nitrogen using standard methodology reported previously (16). Frozen cross sections (8 µm) were cut from the middle third of the TA muscle in the area where the original surgical defect was made. Immunofluorescence stained tissue sections were probed for collagen 1 (1:500; AB755P; Millipore, Billerica, MA), sarcomeric myosin (1:10; MF20; Developmental Studies Hybridoma Bank, Iowa City, IA), laminin (1:200; AB11575; Abcam, Cambridge, MA), CD68 (1:50; MCA341R; AbD Serotec, Raleigh, NC), wheat germ agglutinin (1:20; Alexa Fluor 488 WG; Invitrogen, Grand Island, NY), von Willebrand factor (vWF; 1:200; AB7356; Millipore, Billerica, MA), α-bungartoxin Alexa Fluor 647 (1:100; B35450; Molecular Probes, Grand Island, NY), and nuclei (DAPI; 1:100; Invitrogen). Corresponding Alexaflour 488- and 596-labeled secondary antibodies

(1:200–1:500; Invitrogen) were incubated at room temperature for 1 h. Qualitative assessments of immunostained sections were made by observing three sections (separated by no <160 µm) from three to six muscles per time point per group. For quantification of area, minimum diameter, and circularity of fibers regenerated in the defect area in sedentary and active (runners) rats, laminin-stained sections were analyzed by manually tracing fibers in nonoverlapping images in ImageJ. Additionally, the area fraction of collagen 1 and myosin in the defect area of dual-probed sections were quantified in nonoverlapping images using ImageJ. Red, green, blue channels were separated and then thresholded to remove background. Analyses of fibers in the regenerated area following minced graft repair were performed in three to five muscles per experimental group (sedentary and active).

Sections from contralateral uninjured, nonrepaired, and minced graft-repaired VML-injured muscles stained with hematoxylin and eosin were analyzed for the presence of fibers with centrally located nuclei within the remaining muscle mass. Eight to fifteen nonoverlapping ×20 images of a cross section from the middle of the muscle (within the remaining muscle mass for VML-injured muscles) from three to four muscles from each group at 8 and 16 wk postinjury were analyzed using Image J (National Institutes of Health). Only fibers within the remaining muscle mass were counted. Approximately 1,500 fibers were counted for each group per time point.

Quantitative RT-PCR

RNA was isolated from snap frozen cross sections of TA muscle (3–6 samples per group) that was comprised of both the defect area and the remaining muscle mass (50–100 mg). RNA was extracted using Trizol LS reagent (Invitrogen) and purified using RNeasy mini kit (Qiagen). The yield of RNA was quantified using a NanoDrop spectrometer (NanoDrop Technologies) and optical density (OD)$_{260/280}$ ratios were determined. RNA (500 ng) was reverse transcribed into cDNA using the SuperScript III first-strand synthesis kit (Invitrogen). The primer sets used in the study are listed in Table 1. All primer sets have been synthesized by Sigma-Aldrich DNA oligos design tool. Aliquots (2 µl) of cDNA were amplified with 200 nM forward/reverse primers, SYBR GreenER (Invitrogen) in triplicate using a Bio-Rad CFX96 thermal cycler system (Bio-Rad). Nontemplate control and no reverse transcriptase controls were run for each reaction. Gene expression was normalized to 18S (housekeeping gene) to determine the ΔCT value. Expression levels for each mRNA transcript were determined by the $2^{-\Delta\Delta CT}$ method by normalizing each group (VML or no repair) to its contralateral control, with the exception of comparison made between sedentary and running minced graft groups in which the control legs were not of a similar condition. For these comparisons, gene expression from both the control and VML TA muscle were expressed as $2^{-\Delta CT} \times 10^6$.

Western Blot

The myofibrillar fraction of cross sections that comprised both the defect area and remaining muscle mass of TA muscles (5 muscles per group) was extracted as described previously (14). Protein concentrations were determined with the Pierce BCA protein assay kit (Thermo Scientific). Proteins were resolved by SDS-PAGE using 20 µg of total protein per sample on 4–20% Tris-glycine gels (Bio-Rad). Transfer was made onto nitrocellulose membranes, stained with Ponceau to ensure equal loading, and subsequently blocked for 1 h at room temperature in Tris-buffered saline containing 0.05% (vol/vol) Tween 20 (TBST) and 5% (wt/vol) nonfat dried milk. Membranes were then incubated overnight at 4°C in TBST containing 5% (wt/vol) bovine serum albumin and desmin (Epitomics; Abcam) primary antibody diluted 1:1,000. Membranes were rinsed six times in TBST and then incubated at room temperature for 1 h in TBST and 5% milk containing peroxidase-conjugated goat anti-rabbit secondary antibody diluted 1:3,000. Membranes were rinsed six times in TBST before exposure to ECL Reagents (Invitrogen). The membranes were then

Table 1. *Nucleotide sequence for primers used for quantitative RT-PCR*

Gene	Forward Sequence	Reverse Sequence	Amplicon Length, bp
Collagen 1	5′-CTGGTGAACGTGGTGCAG-3′	5′-GACCAATGGGACCAGTCAGA-3′	123
CCR7	5′-GCTCTCCTGGTCATTTTCCA-3′	5′-AAGCACACCGACTCATACAGG-3′	107
CD163	5′-TCATTTCGAAGAAGCCCAAG-3′	5′-CTCCGTGTTTCACTTCCACA-3′	101
CTGF	5′-CAAGCAGCTGGGAGAACTG-3′	5′-ACAGGGTGCACCATCTTTG-3′	127
TGF-β_1	5′-GTCAGACATTCGGGAAGCA-3′	5′-CCAAGGTAACGCCAGGAAT-3′	138
eMHC	5′-TGGAGGACCAAATATGAGACG-3′	5′-CACCATCAAGTCCTCCACCT-3′	180
MyoD	5′-CGTGGCAGTGAGCACTACAG-3′	5′-TGTAGTAGGCGGCGTCGTA-3′	133
Myogenin	5′-CTACAGGCCTTGCTCAGCTC-3′	5′-GTTGGGACCAAACTCCAGTG-3′	153
Pax7	5′-GCAGTCGGACCACATTCAC-3′	5′-CGCACGACGGTTACTGAAC-3′	155
CD31	5′-ACCTCCAAGCAAAGCAAAGA-3′	5′-GACGGCTGGAGGAGAGTTC-3′	169
Desmin	5′-TACACCTGCGAGATTGATGC-3′	5′-TTAGGTGTCGGATCTCCTCCT-3′	142
Dystrophin	5′-GCCAAAGTTTGAACCAGGAC-3′	5′-ACAGGCCTTTATGCTCATGC-3′	183
18S	5′-GGCCCGAAGCGTTTACTT-3′	5′-ACCTCTAGCGGCGCAATAC-3′	173

CTGF, connective tissue growth factor; TGF-β_1, tranforming growth factor-β_1; eMHC, embryonic myosin heavy chain.

imaged using the Odyssey Fc system (LI-COR Biosciences, Lincoln, NE). The optical density of desmin was normalized to that of the ~42-kDa Ponceau-stained band (28) and used for quantitative analysis.

Statistics

Dependent variables were analyzed using one and two-way ANOVAs or independent samples *t*-tests. Post hoc means comparisons testing was performed when a significant ANOVA was observed. Alpha was set at 0.05. Values are listed as means ± SE. Statistical testing was performed with Prism 6 for Mac (Graphpad, La Jolla CA).

RESULTS

In Vitro Analysis of Minced Grafts

TA muscle tissue was minced into ~1mm^3 pieces using Vanna scissors and placed orthotopically in a volumetric defect in the superior aspect of middle third of the TA (Fig. 1, *A* and *B*). Within each minced tissue, bundles of fragmented muscle fibers with presumptive endomysium and perimysium connective tissue components are present (Fig. 1, *C* and *D*) (26). Minced grafts were cultured on collagen-coated dishes to demonstrate the proliferative capacity of cells emanating from the minced tissue as well as the myogenicity of the explant. Proliferation of cells derived from the minced graft were observed out to 14 days (Fig. 1*E*). Desmin$^+$ cells with characteristic morphology of satellite cells and myotubes were observed on the plate after 5 and 14 days of culture (Fig. 1, *F* and *G*).

Early Response After VML

Immunohistology at the site of injury. Two weeks postinjury, qualitative immunohistological analyses were performed at the site of the defect (Fig. 2, *A–H*). Nonrepaired tissue exhibited
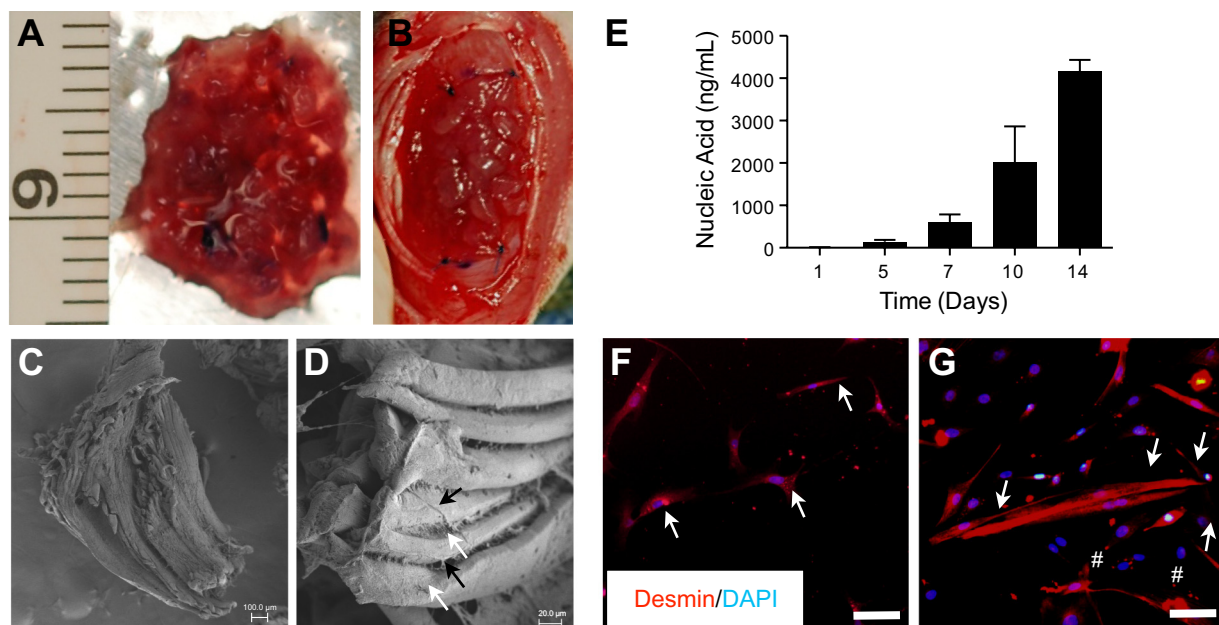

Fig. 1. Minced skeletal muscle graft characterization in vitro. *A* and *B*: minced grafts were created by mincing the superficial portion of the middle third of the tibialis anterior (TA) muscle into ~1-mm^3 pieces. Minced grafts were then placed orthotopically in the fresh wound bed. *C* and *D*: scanning electron microscopy was performed to illustrate the gross structure of minced grafts. In *D*, arrows demarcate perimysium and endomysium connective tissue (white) and neurovascular structures (black). *E*: minced grafts were cultured in vitro to demonstrate that proliferative capacity of resident progenitor cells. Proliferation was analyzed by measuring nucleic acid content over 14 days in culture. *F* and *G*: daughter cells from a single minced graft were probed for desmin protein expression at 5 (*F*) and 14 (*G*) days of culture. Arrows denote desmin-positive myoblasts or myotubes, and # denotes desmin-negative cells.
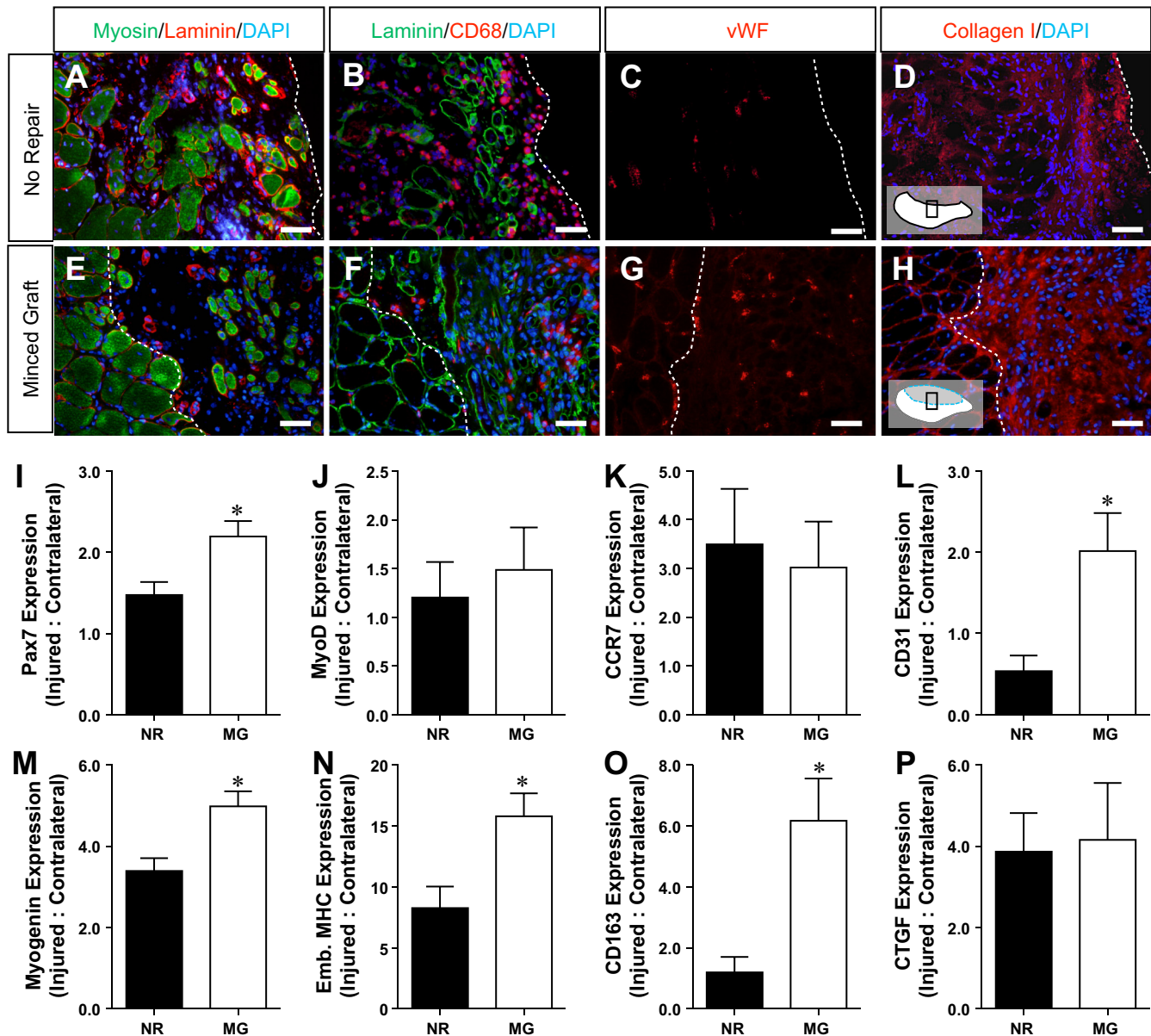
Fig. 2. Promotion of an early regenerative response of volumetric muscle loss (VML) injured muscle with minced graft transplantation. TA muscles were harvested 2 wk postinjury in nonrepaired (NR) and minced graft (MG)-repaired muscles. A–H: defect area was qualitatively analyzed using immunohistochemical staining for myogenesis (myosin, MF20), inflammation (pan-macrophage staining, CD20), vascularization [von Willebrand Factor (vWF)], and extracellular matrix deposition (collagen 1). Three to five muscles per group and per stain were analyzed. Note: diagram of the TA muscle cross section illustrates where the depicted images for each group were captured. White dotted lines denote the approximate interface between the remaining muscle mass (*left*) and the defect area (*right*). Scale bars = 50 µm. I–P: tissue samples comprised of the defect area and the remaining muscle mass were assayed for myogenic (Pax7, MyoD, myogenin, and embryonic myosin heavy chain), inflammatory [M_1 (CCR7) and M_2 (CD163) macrophages], angiogenic (CD31), and extracellular matrix signaling (connective tissue growth factor) gene expression. Values are means ± SE; n = 3–5 per group. *P < 0.05, statistically significant differences between groups.

little evidence of muscle fiber regeneration, marked by the absence of regenerating myosin$^+$ fibers and the formation of a band of connective tissue (collagen 1$^+$), as observed previously (14, 16). In contrast, minced graft-repaired muscles demonstrated signs of de novo muscle fiber regeneration within the defect area, as evidenced by myosin$^+$ fibers, macrophages (CD68$^+$), and vessel formation (vWF$^+$). As observed previously in this model with muscle-derived ECM transplantation (16), the area of macrophage infiltration (CD68$^+$ cells) appeared localized to the defect area for minced graft-repaired

muscles but within the remaining native tissue for nonrepaired muscle. Moreover, collagen 1$^+$ matrix and laminin$^+$ structures were present throughout the defect area in minced graft-repaired muscle, indicating the presence of a putative scaffold for continued regeneration.

Whole muscle gene expression. Expression of genes involved in the early regenerative response of minced graft-repaired and nonrepaired injured muscles was characterized from cross sections of muscle comprised of both the defect area and the remaining muscle mass 2 wk postsurgery (Fig. 2, I–P).

The myogenic response was significantly greater within minced graft-repaired than nonrepaired muscle, as indicated by a greater expression of Pax7, myogenin, and embryonic myosin heavy chain. However, it should be noted that some markers of myogenesis were still upregulated in the nonrepaired tissue (e.g., myogenin and embryonic myosin heavy chain was 3.4- and 8.3-fold greater, respectively, in injured than contralateral uninjured muscles). Expression of CCR7, a marker of M_1 macrophages (58), was upregulated similarly in both groups (~3-fold), while CD163 expression, a marker of M_2 macrophages (48), was only upregulated (~6-fold) in minced graft-repaired muscle, reflective of an M_2 polarization of the infiltrating macrophages (7, 48). CD31, an endothelial cell marker, was also only upregulated in minced graft-repaired muscle (~2-fold). The expression of connective tissue growth factor, a fibrotic marker (56), was upregulated similarly (~4-fold) for both groups.

Prolonged Response After VML

Body and muscle wet weight. There were no differences among group means for body weights at the time of surgery or between groups at 8 and 16 wk postinjury (Table 2). The mean wet weight of the TA muscle VML defect was also similar among all groups (Table 2). TA muscle wet weight for contralateral control muscles was not significantly different between groups at either time point. The wet weight of the TA muscles from the injured leg of the nonrepaired group was significantly reduced by ~12 and 18% at 8 and 16 wk postinjury compared with its contralateral leg, respectively. In contrast, TA muscle weights from the minced graft group were similar between contralateral and injured legs. TA muscles from the injured leg of the minced graft group were significantly heavier than those of the nonrepaired group by ~11 and 21% at 8 and 16 wk postinjury, respectively (Table 2). Eight weeks postinjury EDL muscle weights were similar among all groups. However, 16 wk postinjury EDL muscle weight was increased by ~10% in the injured legs of both nonrepaired and minced graft groups, suggestive of compensatory hypertrophy (46).

Anterior crural muscle torque. Maximal isometric torque (150 Hz) of the anterior crural muscles was measured bilaterally at 8 and 16 wk postinjury (Table 2). At these times, torque produced by contralateral control muscles was similar between nonrepaired and minced graft groups. At 8 wk postinjury, there tended to be a significant improvement in torque produced by the injured leg for the minced graft compared with the nonrepaired group ($P = 0.06$). At 16 wk postinjury, maximal torque for the injured leg was significantly greater for the minced graft group (Table 2).
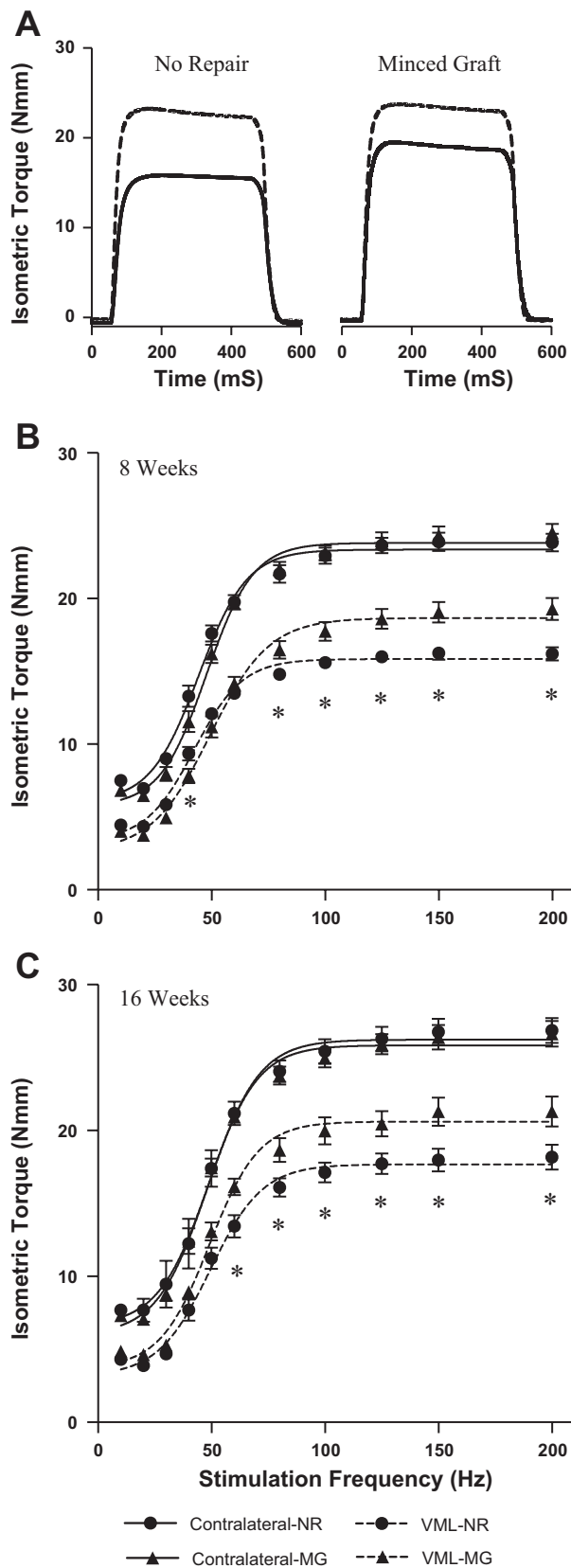
Isolated TA muscle torque. Because the VML injury was created only in the TA muscle, its synergists (EDL and EHL muscles) were distally tenotomized to allow for in vivo torque assessment of the TA muscle in isolation. TA muscle isometric torque was assessed bilaterally as a function of stimulation frequency at 8 and 16 wk postinjury. Within each time point, there were no differences among contralateral control values at any stimulation frequency between groups (Fig. 3 and Table 2). However, at both time points postinjury the injured leg of the minced graft group generated greater submaximal and maximal tetanic torques (8–20%) than those of the nonrepaired group,

Table 2. *Morphological and in vivo functional characteristics*

| | Eight Weeks Postinjury | | | | | | Sixteen Weeks Postinjury | | | |
| | No Repair-Sedentary | | Minced Graft-Sedentary | | Minced Graft-Runner | | No Repair-Sedentary | | Minced Graft-Sedentary | |
	Contralateral	VML	Contralateral	VML	Contralateral	VML	Contralateral	VML	Contralateral	VML
Sample size	6		9		7		5		7	
Body weight at surgery, g	344 ± 2		350 ± 4		332 ± 4		332 ± 3		335 ± 3	
Body weight at death, g	416 ± 3		423 ± 5		372 ± 9‡		453 ± 8		480 ± 11	
TA muscle weight, mg	713 ± 20	625 ± 30*	724 ± 27	696 ± 14†	653 ± 25‡	622 ± 16‡	710 ± 16	584 ± 18*	755 ± 20	709 ± 14†
TA muscle weight:body weight, mg/g	—	—	1.70 ± 1.1	1.64 ± 0.02	1.76 ± 0.06	1.67 ± 0.02	—	—	—	—
EDL muscle weight, mg	167 ± 3	174 ± 9	172 ± 6	182 ± 10	161 ± 4	181 ± 8	173 ± 3	191 ± 8*	182 ± 4	201 ± 5*
TA muscle VML defect weight, mg	—	110 ± 3	—	108 ± 3	—	97.4 ± 1	—	100 ± 1	—	107 ± 7
In vivo maximal isometric tetanic torque										
Anterior crural muscles intact (150 Hz)										
N/mm	30.1 ± 0.7	21.9 ± 0.6*	30.7 ± 0.7	24.0 ± 0.9*	29.2 ± 1.6	24.5 ± 0.9	32.7 ± 1.3	24.4 ± 0.8*	32.8 ± 1.0	27.7 ± 0.9*†
N×mm⁻¹×kg body wt⁻¹	—	—	43.0 ± 1.1	38.8 ± 2.1*	44.8 ± 1.9	39.4 ± 1.0*	—	—	—	—
TA muscle isolated (150 Hz)										
N/mm	23.9 ± 0.6	16.3 ± 0.4*	24.3 ± 0.6	19.1 ± 9*†	23.7 ± 1.3	18.9 ± 1.1*	26.8 ± 0.9	18.0 ± 0.8*	26.4 ± 0.8	21.3 ± 1.0*†
N×mm⁻¹×kg TA wet wt⁻¹	33.6 ± 0.5	26.3 ± 1.3*	33.8 ± 0.8	26.8 ± 1.1*	36.3 ± 1.3	30.3 ± 1.2*‡	37.7 ± 0.7	30.8 ± 1.2*	35.0 ± 0.7	30.0 ± 1.2*
N×mm⁻¹×kg body wt⁻¹	57.4 ± 1.1	39.1 ± 1.3*	57.2 ± 1.2	44.0 ± 1.3*†	63.6 ± 2.8‡	50.8 ± 2.4*‡	59.1 ± 0.9	39.7 ± 1.7*	55.0 ± 1.0	44.4 ± 1.7*†

Values are means ± SE. VML, volumetric muscle loss; TA, tibialis anterior; EDL, extensor digitorum longus. *$P < 0.05$, respective contralateral; †$P < 0.05$, no repair within respective time point. ‡$P < 0.05$, minced graft-sedentary.

Fig. 3. Minced grafts improve in vivo TA muscle torque during the months after VML. TA muscle torque was assessed in vivo following distal extensor digitorum longus (EDL) tenotomy (see METHODS). *A*: representative maximal isometric torque (150 Hz) responses (16 wk postinjury) and torque-frequency curves at 8 (*B*) and 16 (*C*) wk postinjury are presented for the contralateral and VML-injured legs of NR and MG-repaired groups. Values are means ± SE; Sample sizes are listed in Table 2. *$P < 0.05$, statistically significant differences between NR and MG-repaired groups for the VML-injured leg response. All VML responses, regardless of group, were lesser than contralateral values.

as indicated in Fig. 3. All injured leg values regardless of group or time postinjury were significantly less than contralateral control values. Nonrepaired and minced graft-repaired VML-injured muscles increased maximal torque from 8 and 16 wk postinjury at similar rate as their contralateral control muscles (Table 2). Of note, maximal isometric tetanic torque when normalized to TA muscle weight (a crude estimate of specific torque) was similar for the injured leg between nonrepaired and minced graft groups at both time points, and all injured leg values were significantly reduced compared with contralateral control muscle (Table 2).

Following isometric testing, a subset of rats at 16 wk postinjury performed isokinetic functional testing (Fig. 4). There were no differences between groups at any contraction velocity for the contralateral control leg. However, for the injured leg the minced graft group produced ∼21–26% greater isokinetic torque from 400 to −400°/s than nonrepaired muscles. Interestingly, the portion of the functional deficit restored appeared to increase from shortening to lengthening velocities (e.g., 400°/s vs. −400°/s; ∼36 vs. 51% of the torque deficit was restored), potentially reflecting a greater number of active myosin-actin interactions that are available to bind during lengthening contractions (33) following regeneration. The injured muscles of the minced graft group performed significantly more work (mJ) than those of the nonrepaired group during 200 to −400°/s isokinetic contractions (Fig. 4*B*) and produced significantly more average power during the −400°/s isokinetic contraction (Fig. 4*C*).

Histology at the site of VML. Representative TA muscle cross sections from uninjured, nonrepair, and minced graft-repaired groups 16 wk postinjury are presented in Fig. 5. Qualitatively, VML resulted in smaller cross sectional area of the tissue (which agrees with the gross morphology of the tissue we observed at harvest). In minced graft-repaired muscle an area of regenerated tissue is present in the superior portion of the TA muscle, where the defect was originally made. Immunohistological observations of the defect area indicated that little to no muscle fiber regeneration occurred in nonrepaired muscle at 8 and 16 wk postinjury, as previously reported (16). In contrast, minced graft-repaired muscles appeared with the following characteristics: marked regeneration of muscle fibers within the original defect area at 8 (Fig. 5*C*) and 16 (Fig. 5, *D* and *E*) wk postinjury that approximated the size of native fibers reported in the literature (3, 16) by 8 wk postinjury (Fig. 9*E*, sedentary ≈2,300 μm²) but were not always oriented along the same plane as the adjacent remaining muscle fibers (e.g., Fig. 5*E*). Additionally, there was an increased collagen 1 presence surrounding the regenerated fibers (see Fig. 9*I*, sed-
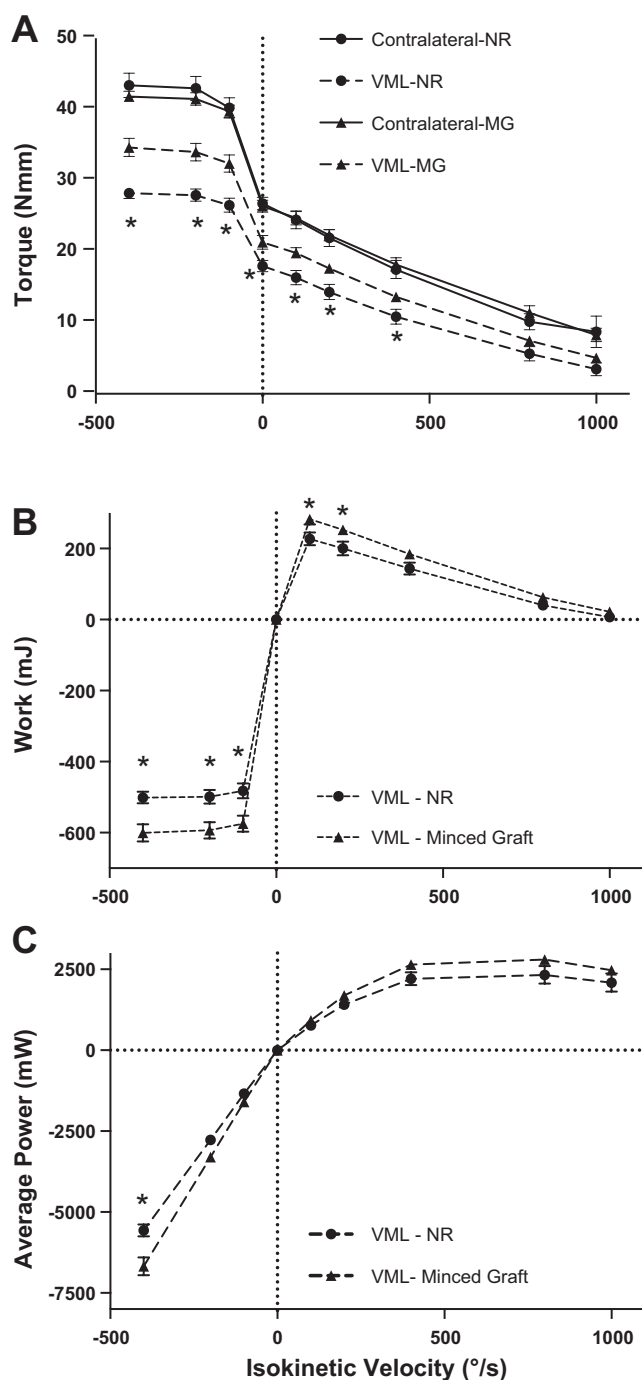
Fig. 4. In vivo TA muscle isokinetic torque is partially restored with minced graft transplantation. TA muscle isokinetic torque measurements were performed 16 wk after VML injury and with the EDL muscle distally tenotomized. *A*: torque as a function of isokinetic velocity was measured in contralateral and injured limbs from NR and MG-repaired rats. *B* and *C*: work (mJ) performed (*B*) and average power (mW) (*C*) produced during isokinetic contractions are presented for the injured legs of each group. Values are means ± SE; $n = 4$ per group. *$P < 0.05$, statistically significant differences between NR and MG-repaired groups for the VML-injured leg response. All VML responses, regardless of group, were lesser than contralateral values.

entary). Lastly, out to 16 wk postinjury there were fibers located within the defect area with centrally located nuclei, indicating that regenerative and potentially remodeling events were still occurring (Fig. 5*D*).

Innervation of regenerated fibers. An important question related to the contribution of regenerated muscle fibers in the area defect to net torque production (Figs. 3 and 5) is that of innervation. Motor endplates (i.e., α-bungarotoxin staining of a grouping of acetylcholine receptors) were consistently observed on muscle fibers within the defect area by 8 wk postinjury (Fig. 6, *A* and *B*). To determine if the fibers were innervated and able to contribute to net torque production, the common peroneal nerve was repeatedly stimulated to deplete the glycogen within innervated muscle fibers in minced graft-repaired muscle (Fig. 6, *C–H*). Compared with nonstimulated muscles, fibers in the remaining muscle mass and the defect area were significantly and similarly depleted of glycogen following stimulation (Fig. 6*D*). These results indicate that the muscle fibers that regenerated in the defect area are innervated.

Prolonged injury in the remaining muscle mass. We have previously observed that in nonrepaired muscle the remaining muscle mass after VML exhibits signs of muscle injury out to 16 wk postinjury, presumably due to secondary overload injury (16, 71). In this study, analysis of standard hematoxylin and eosin images indicated that ~30% of fibers in the remaining muscle mass of nonrepaired muscle contained centrally located nuclei, compared with only ~7% for minced graft-repaired muscle (Fig. 7).

To further characterize the impact of VML on the remaining tissue of nonrepaired muscles, and to determine if transplantation of minced grafts ameliorates these effects, gene expression analyses were performed on cross sections of muscle comprised of both the defect area and the remaining muscle mass. At both 8 and 16 wk postinjury, gene expression for the structural proteins desmin and dystrophin was significantly upregulated in nonrepaired (~3–8 fold compared with contralateral muscle) compared with minced graft-repaired muscle (Fig. 8, *A* and *B*). However, desmin protein content was not significantly different between control and VML-injured muscle of either experimental group (Fig. 8, *D–F*), suggesting that desmin protein synthesis is upregulated to match increased rates of degradation. Further, tranforming growth factor-β_1 (TGF-β_1) expression was upregulated (~4- to 5-fold) at 8 wk postinjury for both groups, but remained upregulated only for nonrepaired tissue 16 wk postinjury (~4-fold; Fig. 8*C*), suggestive of continued fibrosis secondary to functional overload in nonrepaired tissue (52, 56).

Impact of Voluntary Wheel Running on Minced Graft Regeneration

Although transplantation of minced grafts promoted significant de novo muscle fiber regeneration within the defect site, the contribution of these fibers to net torque production is likely suboptimal based on the histomorphological observations above. In support, maximal isometric torque normalized to muscle wet weight (N·mm^{-1}·g^{-1}) was not significantly improved with minced graft repair compared nonrepaired tissue (Table 2). In an effort to improve the histomorphology of the tissue regenerated in the defect area due to graft transplantation, rats were given access to running wheels starting 7 days after VML injury and until 8 wk postinjury.

The rats ran on average ~1,800 m/day (Fig. 9), the result of which was a smaller phenotype in terms of body and TA muscle weights (Table 2), as well as a smaller area (~−44%)
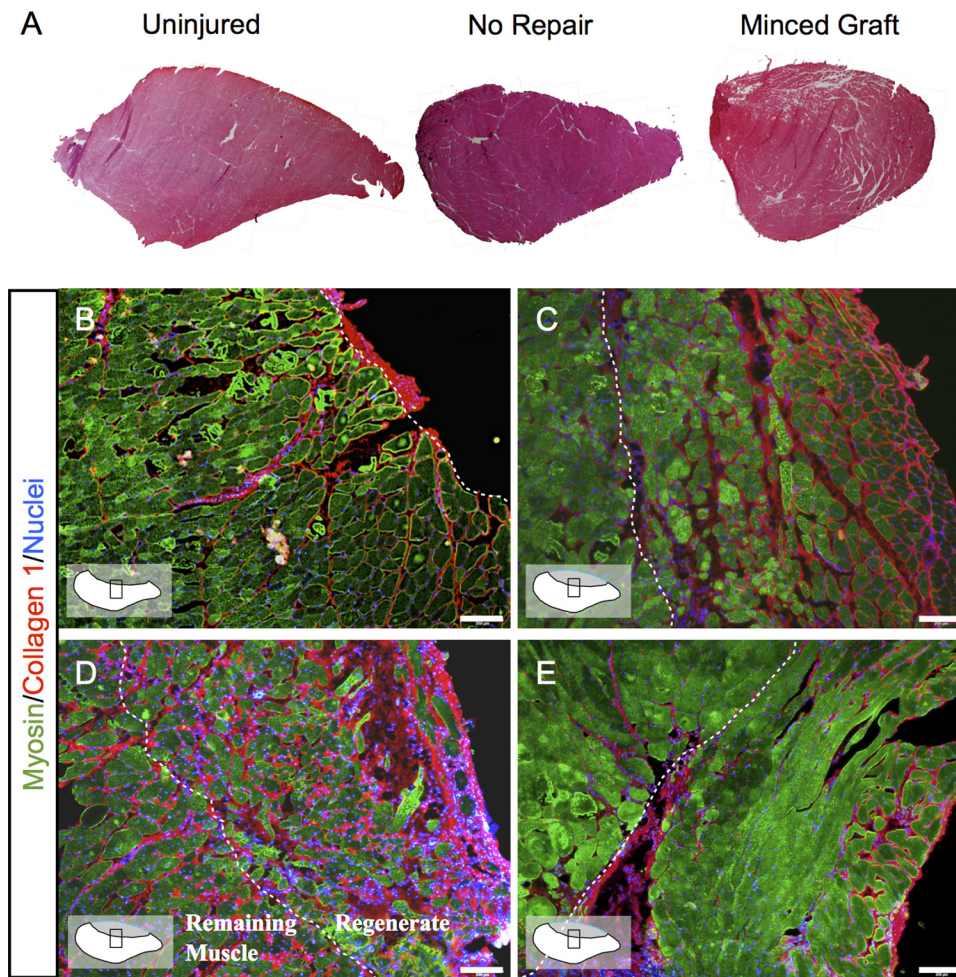
Fig. 5. Minced graft transplants promote de novo skeletal muscle fiber regeneration in VML-injured muscle. *A*: whole TA muscle cross sections from uninjured and VML-injured NR and MG-repaired muscles 16 wk after injury are presented. *B–E*: TA muscle cross sections probed for myosin (MF20) and collagen 1 were qualitatively analyzed for tissue regeneration in the defect area. Muscles were harvested from NR (*B*) and MG-repaired muscles at 8 (*C*) and 16 wk (*D* and *E*) postinjury. Four to six muscles per group and time were analyzed. Note: diagram of the TA muscle cross section illustrates where the depicted images for each group were captured. White dotted lines denote the approximate interface between the remaining muscle mass (*left*) and the defect area (*right*). Scale bars = 200 μm.

and diameter ($\sim-23\%$) of regenerated fibers at the defect site (Fig. 9). Of note, the regenerated fiber area and diameter in sedentary rats were similar to values previously reported (3, 16). It is possible that the reduced fiber area is in part due to a greater fiber pennation angle in the runners; however, this seems unlikely since the circularity of the muscle fibers was not different between groups ($P = 0.572$). The regenerated tissue in the defect area presented with less fibrosis following running, as evidenced by a lesser collagen 1 and a greater myosin area fraction per field (Fig. 9). Although not statistically significant ($P = 0.456$), collagen 1 gene expression was $\sim40\%$ less for runner than sedentary minced graft-repaired muscles. Because the inflammatory response is known to mediate regenerative outcomes in skeletal muscle, gene expression of the M_1 and M_2 macrophage markers CCR7 and CD163 was measured 2 wk postinjury (1 wk of running). Both markers were significantly upregulated in control and VML muscles from runner compared with sedentary rats (Fig. 10), suggesting that modulation of the immune response may have played a role in the differential morphological phenotypes. Ultimately, in response to these changes and others that may have occurred in the remaining muscle mass, torque normalized to muscle wet weight was significantly improved after wheel running (Table 2), indicating an improvement in the quality of tissue regenerated after minced graft transplantation.

DISCUSSION

The primary findings of this study are that minced muscle grafts transplanted to a fresh wound bed after VML promote remarkable skeletal muscle fiber regeneration by 8 and out to 16 wk postinjury, reminiscent of that observed previously for whole muscle regeneration [see Fig. 1 in Carlson and Gutmann (12)]. The fibers regenerated in the defect area (Fig. 5) were innervated by 8 wk postinjury, as determined in a glycogen depletion study (Fig. 6) and had a similar cross-sectional area (Fig. 9, sedentary) as uninjured muscle fibers reported in the literature (16). Ultimately, minced graft transplantation improved whole muscle functional capacity, restoring up to $\sim55\%$ of the functional deficit present in nonrepaired muscle (Figs. 3 and 4; Table 2).

Comparison of the therapeutic benefit of other treatments tested in VML models that vary in muscle type, defect geometry, or animal species and strain is difficult (e.g., Refs. 14, 37). With that in mind, in a TA muscle VML injury in immune competent mice (C57BL/6J), Rossi et al. (47) reported comparable relative ($\sim50\%$ recovery of deficit) results with transplantation of freshly isolated satellite cells encapsulated in a hydrogel. However, it is worth noting that in the current study minced graft transplantation resulted in an improvement in maximal isometric torque (3.3 N/mm) that is similar to that of the entire mouse anterior crural muscle
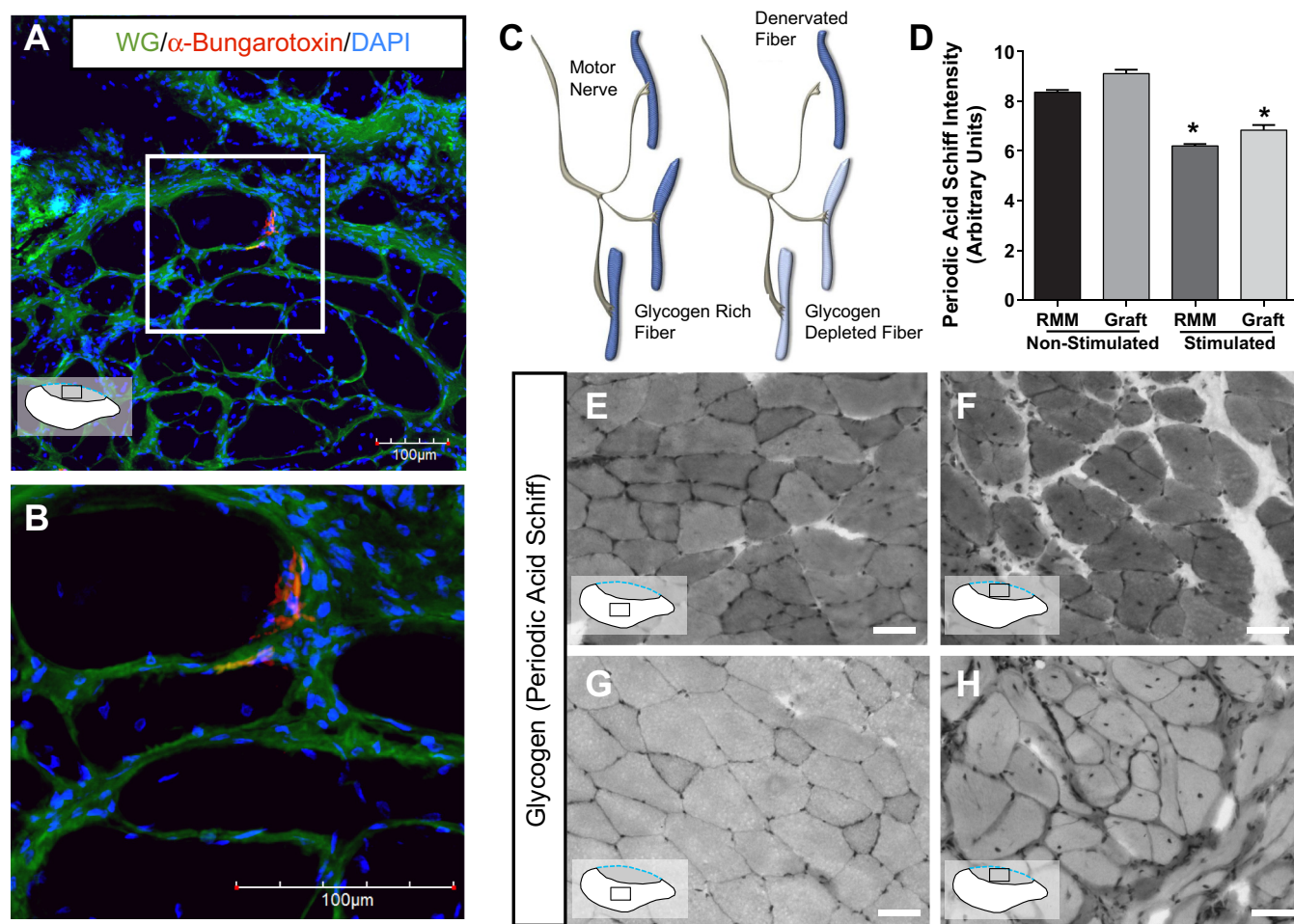
Fig. 6. Regenerated muscle fibers in the defect area after minced graft transplantation are innervated. *A* and *B*: TA muscle sections from MG-repaired muscles probed with α-bungarotoxin and wheat germ agglutinin were analyzed for the presence of motor endplates on muscle fibers within the defect area. Image in *A* was captured using confocal microscopy with a $\times$10 objective. Image in *B* is digitally zoomed from the area within the white box in *A*. Scale bars = 100 μm. *C–H*: glycogen depletion of muscle fibers following repetitive common peroneal nerve stimulation was performed to determine if muscle fibers in the regenerated of MG-repaired muscles are innervated. *C*: illustrates a conceptual schematic of the procedure. *D*: quantification of glycogen content (period acid-Schiff-stained sections) within muscle fibers of the remaining muscle mass (RMM; *E* and *G*) and MG area (*F* and *H*) in nonstimulated (*E* and *F*) and stimulated muscles (*G* and *H*). Values are means ± SE; $n = 3$ per group. *$P < 0.05$, statistically significant differences from respective nonstimulated muscle values. Scale bars for *E–H* = 200 μm.

unit (15). In the same VML model as used in the current study, we recently demonstrated that transplantation of a decellularized muscle-derived ECM failed to support de novo muscle fiber regeneration and instead remodeled into fibrotic tissue. Interestingly, the transplanted ECM still promoted functional recovery (~20% of functional deficit) out to 16 wk postinjury, which was attributed to either an improved transmission of force or a protective effect of the ECM on the remaining muscle mass (16). Given the approximately twofold greater functional recovery observed in the current study, it is clear that the functional improvements are not simply due to a "bridging" effect but rather an increase in functional tissue.

It is likely that the muscle fibers that regenerated in the defect area contributed suboptimally to net torque production in minced graft-repaired sedentary rats, due to the increased presence of ECM deposition (collagen 1$^+$) and in some instances improper fiber orientation (Figs. 5 and 9). These observations reflect those previously made by Carlson and Gutmann (12), wherein whole regenerated rat gastrocnemius muscle from minced grafts did not

appear to transmit forces efficiently, but is in contrast to those observed in the mouse (49) in which overt fibrosis in the regenerate was not observed. In fact, the ECM material in regenerated tissue in the defect area appears strikingly similar to soleus muscle following repeated bouts of strain (53), suggesting a shared mechanism in promoting this phenotype (e.g., prolonged inflammatory response or TGF-β_1 signaling; Fig. 8). In an attempt to improve the histomorphology of the regenerated tissue, a subset of rats in this study were given access to voluntary running wheels. Although this mode of exercise may not be the most clinically relevant, running activity has been shown previously to improve regeneration following toxin-induced injury (61) and to increase protein content and/or muscle mass of whole soleus muscle grafts (19, 68) and tissue regenerated from minced gastrocnemius muscle (66). To this effect, wheel running altered the phenotype of the regenerated fibers, marked by a reduced collagen 1 content in the defect area. Additionally, the regenerated fibers were on average significantly smaller than in sedentary animals (Fig. 9), which may reflect a protective mechanism to mechanical stress (27, 39, 53). Regardless, these changes in morphology, along with poten-
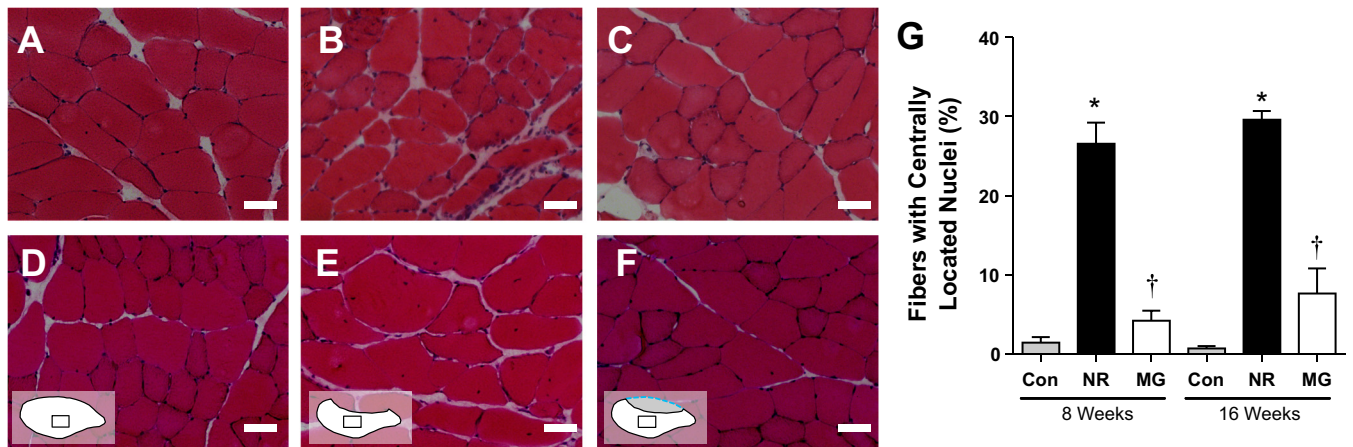
Fig. 7. Remaining muscle mass of NR VML-injured muscle presents with chronic injury. Contralateral (Con; *A* and *D*) and VML-injured muscles (*B*, *C*, *E*, and *F*) from NR (*B* and *E*) and MG (*C* and *F*) groups at 8 (*A–C*) and 16 (*D–F*) wk postinjury were analyzed (*G*) for the presence of centrally located nuclei in hematoxylin and eosin-stained sections. Only muscle fibers in the remaining muscle mass were included in the analysis. Scale bars = 50 μm. Values are means ± SE; $n = 3–4$ muscles per group. Within each time point, $*P < 0.05$, NR ≠ Con; $P < 0.05$, MG ≠ Con and NR.

tially others in the remaining muscle mass, promoted a significant improvement in isometric torque when normalized to body weight and muscle weight (Table 2), suggesting an improved contribution of the regenerated muscle fibers to net torque.

The early host response to transplanted materials determines successful tissue regeneration. This has long been recognized, as Hoja in 1958 (24) postulated that nonautologous muscle grafts fail at the time when revascularization allows for im-
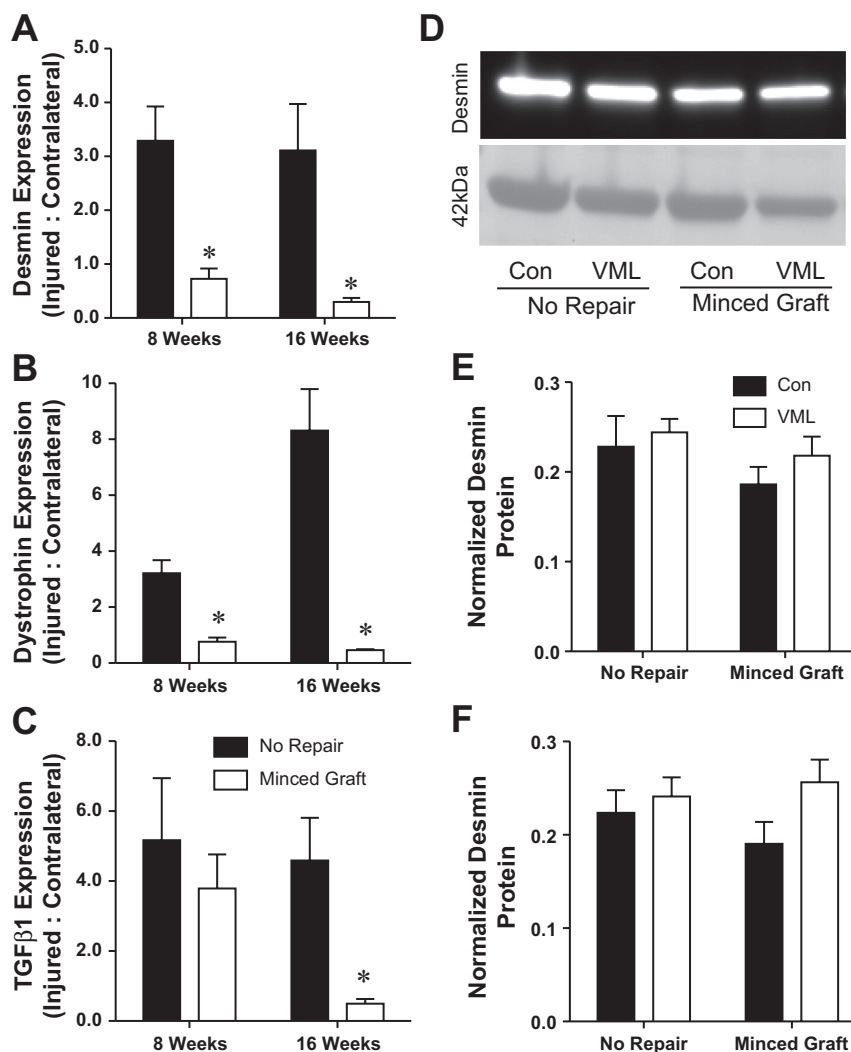

Fig. 8. Gene expression of structural proteins and transforming growth factor-β_1 (TGF-β_1) are chronically upregulated in NR VML-injured muscle. *A–C*: 8 and 16 wk postinjury, TA muscle samples from NR and MG-repaired muscles that were comprised of the defect area and the remaining muscle mass were assayed for desmin, dystrophin, TGF-β_1 gene expression; $n = 3–5$ samples per group. *D* and *E*: protein isolated from these tissues were probed for desmin protein content via Western blot. Desmin protein optical density was normalized to a 42-kDa band visualized on the membrane using Ponceau. There were no statistical differences among contralateral and VML-injured samples from NR or MG-repaired rats at 8 (*E*) or 16 (*F*) wk postinjury; $n = 5$ muscles per group. Values are means ± SE. $*P < 0.05$, statistically significant differences between groups.
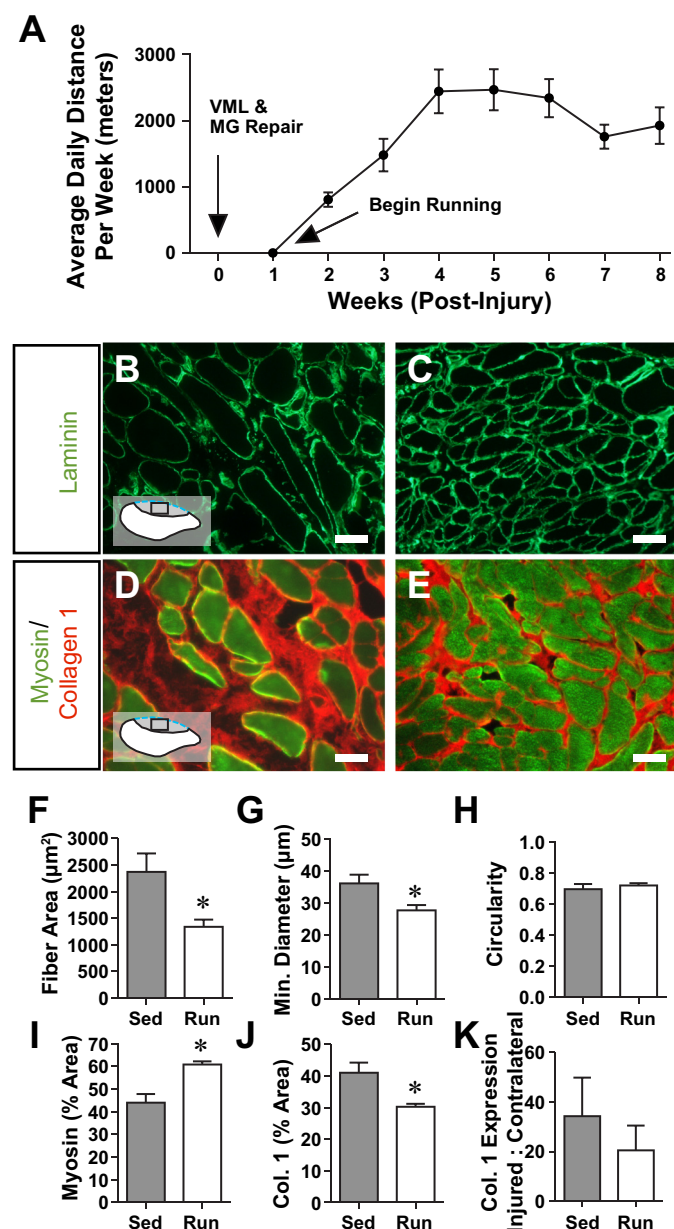
Fig. 9. Voluntary wheel running reduces the extracellular matrix content among fibers regenerated from minced grafts. *A*: subset of MG-repaired rats were given access to voluntary running wheels one wk after injury and were allowed to run for 1 or 7 wk. Eight week postinjury sections from MG-repaired TA muscles from sedentary (*B* and *D*) and runner (*C* and *E*) rats were probed for laminin or collagen 1 and myosin. The ×20 nonoverlapping images from the defect area of 3–5 muscles from each group were analyzed for fiber area (*F*), minimum ferret's diameter (*G*), circularity (*H*; laminin sections) and relative area of myosin (*I*), and collagen 1 (*J*; myosin and collagen 1 sections). Note: Only regenerated tissue within the defect area was included for analysis. *K*: collagen 1 gene expression was measured in tissue samples comprised of the defect area and the remaining muscle mass from the muscle described above; $n = 4–6$ per group. Values are means ± SE. *$P < 0.05$, significant differences between sedentary and running conditions.

(11) described minced grafts of a whole gastrocnemius muscle during the second week after transplantation as being marked by myogenic regeneration and the formation of new ECM macrophages and other mononuclear monocytes were observed among the regenerating tissue. Our 2-wk postinjury observations of minced grafts transplanted in a wound bed are in line with these findings (Fig. 2). Additionally, we observed that the muscles repaired with minced grafts presented with an M_2 macrophage polarization, as determined by gene expression, which coincided with an upregulation of myogenic (e.g., myogenin) and angiogenic (e.g., CD31) gene expression and ECM deposition (Fig. 2). These findings are in accordance with a recent report indicating that successful constructive remodeling of biological ECMs are related to M_2 macrophage polarization 2 wk after transplantation (7). Interestingly, voluntary wheel running appeared to modulate the acute immune response in minced graft-repaired muscles (Fig. 10) by increasing gene expression of M_1 (CCR7) and M_2 (CD163) macrophages,
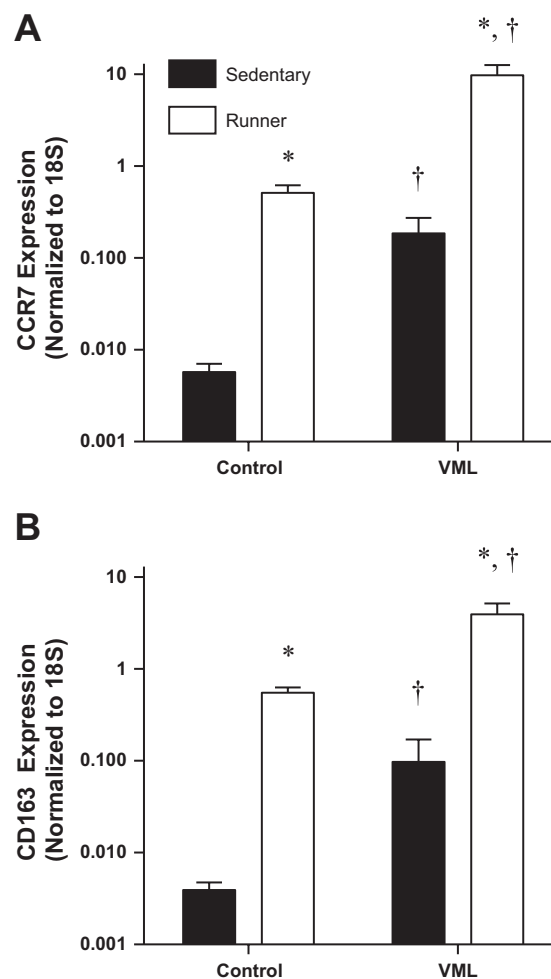

Fig. 10. Early inflammatory response in MG-repaired muscles is augmented with voluntary wheel running. TA muscles from sedentary and active (1 wk of running) MG-repaired muscles were harvested 2 wk postinjury. Tissue samples comprised of the defect area and the remaining muscle mass were assayed for gene expression of M_1 (*A*; CCR7) and M_2 (*B*; CD163) macrophage markers. Values are means ± SE; $n = 5–6$. *$P < 0.05$, significant differences between runner and sedentary rats in contralateral control or VML-injured muscles. †$P < 0.05$, significant differences between contralateral control or VML-injured muscle within an activity status.

mune cell invasion. In regards to regeneration, macrophage activity is crucial for the repair of injured skeletal muscle (67) and, more specifically, distinct macrophage populations (M_1 and M_2) have been shown to, respectively, mediate the degenerative and regenerative events after injury (3, 48). Carlson

which corresponded with an apparent improvement in myogenesis (i.e., greater myosin per collagen content in the defect area; Fig. 9). Further study may be warranted to address immune modulation for the betterment of functional outcomes with minced graft repair.

Orthopedic care for extremity trauma focuses primarily on bone healing and mitigation of infection, with soft tissue therapies being considered later, if at all. In previous preclinical studies of VML, little attention has been given to the "health" of the muscle left after VML, instead focusing on aberrant regeneration in the defect area. Previously with this VML model, we made qualitative observations of prolonged (out to 16 wk) muscle fiber injury and documented increased fibrosis in the remaining muscle mass (16), which was presumed to result from functional overload. Similarly, in the current study ~30% of the muscle fibers in nonrepaired muscle had centrally located nuclei 16 wk postinjury (Fig. 7), suggesting that the remaining muscle is undergoing chronic cycles of degeneration and regeneration. In support, TGF-β_1 expression was upregulated at 8 and 16 wk postinjury in nonrepaired tissue, the chronic activity of which plays a role in developing fibrosis and inhibiting myogenesis in dystrophic muscle (1, 4). In addition, at these prolonged time points, gene expression for the structural proteins dystrophin and desmin, which would likely be damaged in response to functional overload (29), was also upregulated without repair. Moreover, 2 wk postinjury the nonrepaired muscle exhibited extensive damage localized within the remaining muscle mass near the defect area marked by macrophage invasion (CD68$^+$ cells) and muscle fiber disruption (Fig. 2). Given that this VML model only removes ~20% of the TA muscle, it is likely that more severe VML would exacerbate this potentially myopathic phenotype. Interestingly, transplantation of minced grafts ameliorated this response. It is unclear if the minced graft treated or protected, potentially by providing trophic factors or mechanical stability, respectively, the remaining muscle mass from chronic injury. However, these results do highlight the need for an early intervention to treat VML.

Given the limited treatment options available for VML (22), the clinical relevance of the current treatment modality should be addressed. When considering compromised bone regeneration, bone autograft, most commonly derived from the iliac crest, has long been the gold standard (51). This strategy is effective and because biologically relevant material compatible with and beneficial for its intended application is applied, i.e., bone autograft contains osteogenic, osteoconductive, and osteoinductive elements that are critical for improving bone regeneration (51). With the use of bone as a corollary, it can be argued that the skeletal muscle autograft approach supplies myoconductive, myoinductive, and myogenic elements conducive to improved muscle regeneration. For example, the ECM may facilitate progenitor cell attachment (54) and thus be considered myoconductive. Growth factors associated with skeletal muscle extracellular matrixes and within mature muscle fibers could all act as inductive agents (59, 70). The myogenic component may be attributed largely to the delivery of satellite cells delivered within their niche, similar to that reported by Collins et al. (13) where the transplantation of single fibers resulted in a substantial satellite cell delivery. As it relates to the current study, the delivery of minced muscle is essentially the delivery of bundles of single fibers; therefore, it then follows that there was a considerable transfer of satellite cells. This association (myogenic cell delivery via minced muscle fragments) was also exploited by Bierinx and Sebille (5) as a clinically relevant means to prevent incontinence. A limitation in the current study is the use of the portion of the muscle explanted to create the VML as the source for minced grafts. The clinical translation of minced grafts for the treatment of large VML injuries will require the selection of a donor site and consideration of its morbidity, which will be addressed in future studies.

As with bone regeneration where osteoconductive, osteoinductive, or osteogenic substitutes or adjuncts are being developed, a substantial effort has been and will continue to be directed towards developing substitutes for myoconductive, myoinductive, and myogenic elements for VML repair. However, as opposed to that described for bone injury where autograft represents the standard to which other developments are compared (51), no such standard currently exists for the volumetric loss of skeletal muscle. Herein we provide compelling data to suggest that the autologous transfer of minced skeletal muscle is an appropriate standard for the future advancement of VML therapies.

DISCLOSURES

No conflicts of interest, financial or otherwise, are declared by the author(s). The opinions or assertions contained herein are the private views of the author and are not to be construed as official or as reflecting the views of the Department of the Army or the Department of Defense.

AUTHOR CONTRIBUTIONS

Author contributions: B.T.C. and C.R.R. conception and design of research; B.T.C., K.G., and C.L.W. performed experiments; B.T.C., K.G., C.L.W., and J.S.M. analyzed data; B.T.C., K.G., C.L.W., J.S.M., T.J.W., and C.R.R. interpreted results of experiments; B.T.C. prepared figures; B.T.C., K.G., C.L.W., and C.R.R. drafted manuscript; B.T.C., K.G., C.L.W., J.S.M., T.J.W., and C.R.R. edited and revised manuscript; B.T.C., K.G., C.L.W., J.S.M., T.J.W., and C.R.R. approved final version of manuscript.

REFERENCES

1. **Andreetta F, Bernasconi P, Baggi F, Ferro P, Oliva L, Arnoldi E, Cornelio F, Mantegazza R, Confalonieri P.** Immunomodulation of TGF-beta 1 in mdx mouse inhibits connective tissue proliferation in diaphragm but increases inflammatory response: implications for antifibrotic therapy. *J Neuroimmunol* 175: 77–86, 2006.
2. **Armstrong RB, Saubert CW 4th, Sembrowich WL, Shepherd RE, Gollnick PD.** Glycogen depletion in rat skeletal muscle fibers at different intensities and durations of exercise. *Pflügers Arch* 352: 243–256, 1974.
3. **Arnold L, Henry A, Poron F, Baba-Amer Y, van Rooijen N, Plonquet A, Gherardi RK, Chazaud B.** Inflammatory monocytes recruited after skeletal muscle injury switch into antiinflammatory macrophages to support myogenesis. *J Exp Med* 204: 1057–1069, 2007.
4. **Bernasconi P, Torchiana E, Confalonieri P, Brugnoni R, Barresi R, Mora M, Cornelio F, Morandi L, Mantegazza R.** Expression of transforming growth factor-beta 1 in dystrophic patient muscles correlates with fibrosis. Pathogenetic role of a fibrogenic cytokine. *J Clin Invest* 96: 1137–1144, 1995.
5. **Bierinx AS, Sebille A.** Mouse sectioned muscle regenerates following auto-grafting with muscle fragments: a new muscle precursor cells transfer? *Neurosci Lett* 431: 211–214, 2008.

6. **Booth FW, Laye MJ.** Lack of adequate appreciation of physical exercise's complexities can pre-empt appropriate design and interpretation in scientific discovery. *J Physiol* 587: 5527–5539, 2009.

7. **Brown BN, Londono R, Tottey S, Zhang L, Kukla KA, Wolf MT, Daly KA, Reing JE, Badylak SF.** Macrophage phenotype as a predictor of constructive remodeling following the implantation of biologically derived surgical mesh materials. *Acta Biomater* 8: 978–987, 2012.

8. **Burke RE, Levine DN, Tsairis P, Zajac FE 3rd.** Physiological types and histochemical profiles in motor units of the cat gastrocnemius. *J Physiol* 234: 723–748, 1973.

9. **Burns TC, Stinner DJ, Possley DR, Mack AW, Eckel TT, Potter BK, Wenke JC, Hsu JR; Skeletal Trauma Research Consortium.** Does the zone of injury in combat-related type III open tibia fractures preclude the use of local soft tissue coverage? *J Orthop Trauma* 24: 697–703, 2010.

10. **Caldwell CJ, Mattey DL, Weller RO.** Role of the basement membrane in the regeneration of skeletal muscle. *Neuropathol Appl Neurobiol* 16: 225–238, 1990.

11. **Carlson BM.** Regeneration for the completely excised gastrocnemius muscle in the frog and rat from minced muscle fragments. *J Morphol* 125: 447–472, 1968.

12. **Carlson BM, Gutmann E.** Development of contractile properties of minced muscle regenerates in the rat. *Exp Neurol* 36: 239–249, 1972.

13. **Collins CA, Olsen I, Zammit PS, Heslop L, Petrie A, Partridge TA, Morgan JE.** Stem cell function, self-renewal, and behavioral heterogeneity of cells from the adult muscle satellite cell niche. *Cell* 122: 289–301, 2005.

14. **Corona BT, Machingal MA, Criswell T, Vadhavkar M, Dannahower AC, Bergman C, Zhao W, Christ GJ.** Further development of a tissue engineered muscle repair construct in vitro for enhanced functional recovery following implantation in vivo in a murine model of volumetric muscle loss injury. *Tissue Eng Part A* 18: 1213–1228, 2012.

15. **Corona BT, Rouviere C, Hamilton SL, Ingalls CP.** FKBP12 deficiency reduces strength deficits after eccentric contraction-induced muscle injury. *J Appl Physiol* 105: 527–537, 2008.

16. **Corona BT, Wu X, Ward CL, McDaniel JS, Rathbone CR, Walters TJ.** The promotion of a functional fibrosis in skeletal muscle with volumetric muscle loss injury following the transplantation of muscle-ECM. *Biomaterials* 34: 3324–3335, 2013.

17. **Criswell TL, Corona BT, Ward CL, Miller M, Patel M, Wang Z, Christ GJ, Soker S.** Compression-induced muscle injury in rats that mimics compartment syndrome in humans. *Am J Pathol* 180: 787–797, 2012.

18. **Cross JD, Ficke JR, Hsu JR, Masini BD, Wenke JC.** Battlefield orthopaedic injuries cause the majority of long-term disabilities. *J Am Acad Orthop Surg* 19, Suppl 1: S1–7, 2011.

19. **Esser KA, White TP.** Prior running reduces hypertrophic growth of skeletal muscle grafts. *J Appl Physiol* 69: 451–455, 1990.

20. **Faulkner JA, Markley JM Jr, McCully KK, Watters CR, White TP.** Characteristics of cat skeletal muscles grafted with intact nerves or with anastomosed nerves. *Exp Neurol* 80: 682–696, 1983.

21. **Gillani S, Cao J, Suzuki T, Hak DJ.** The effect of ischemia reperfusion injury on skeletal muscle. *Injury* 43: 670–675, 2012.

22. **Grogan BF, Hsu JR.** Volumetric muscle loss. *J Am Acad Orthop Surg* 19, Suppl 1: S35–37, 2011.

23. **Hall JK, Banks GB, Chamberlain JS, Olwin BB.** Prevention of muscle aging by myofiber-associated satellite cell transplantation. *Sci Transl Med* 2: 57ra83, 2010.

24. **Hoja S.** [Contribution to the question of nourishment of muscle transplants after auto-, homo, and hetero-transplantation]. *Biologia (Bratislava)* 13: 514–522, 1958.

25. **Huijing PA, Jaspers RT.** Adaptation of muscle size and myofascial force transmission: a review and some new experimental results. *Scand J Med Sci Sports* 15: 349–380, 2005.

26. **Jarvinen TA, Jozsa L, Kannus P, Jarvinen TL, Jarvinen M.** Organization and distribution of intramuscular connective tissue in normal and immobilized skeletal muscles. An immunohistochemical, polarization and scanning electron microscopic study. *J Muscle Res Cell Motil* 23: 245–254, 2002.

27. **Karpati G, Carpenter S, Prescott S.** Small-caliber skeletal muscle fibers do not suffer necrosis in mdx mouse dystrophy. *Muscle Nerve* 11: 795–803, 1988.

28. **Klein D, Kern RM, Sokol RZ.** A method for quantification and correction of proteins after transfer to immobilization membranes. *Biochem Mol Biol Int* 36: 59–66, 1995.

29. **Lehti TM, Kalliokoski R, Komulainen J.** Repeated bout effect on the cytoskeletal proteins titin, desmin, and dystrophin in rat skeletal muscle. *J Muscle Res Cell Motil* 28: 39–47, 2007.

30. **Lepper C, Partridge TA, Fan CM.** An absolute requirement for Pax7-positive satellite cells in acute injury-induced skeletal muscle regeneration. *Development* 138: 3639–3646, 2011.

31. **Lim AY, Lahiri A, Pereira BP, Tan JA, Sebastin SJ, Tan BL, Zheng L, Prem Kumar V.** The role of intramuscular nerve repair in the recovery of lacerated skeletal muscles. *Muscle Nerve* 33: 377–383, 2006.

32. **Lin CH, Lin YT, Yeh JT, Chen CT.** Free functioning muscle transfer for lower extremity posttraumatic composite structure and functional defect. *Plast Reconstr Surg* 119: 2118–2126, 2007.

33. **Linari M, Lucii L, Reconditi M, Casoni ME, Amenitsch H, Bernstorff S, Piazzesi G, Lombardi V.** A combined mechanical and X-ray diffraction study of stretch potentiation in single frog muscle fibres. *J Physiol* 526: 589–596, 2000.

34. **Lowe DA, Warren GL, Ingalls CP, Boorstein DB, Armstrong RB.** Muscle function and protein metabolism after initiation of eccentric contraction-induced injury. *J Appl Physiol* 79: 1260–1270, 1995.

35. **Maltin CA, Harris JB, Cullen MJ.** Regeneration of mammalian skeletal muscle following the injection of the snake-venom toxin, taipoxin. *Cell Tissue Res* 232: 565–577, 1983.

36. **Mase VJ Jr, Hsu JR, Wolf SE, Wenke JC, Baer DG, Owens J, Badylak SF, Walters TJ.** Clinical application of an acellular biologic scaffold for surgical repair of a large, traumatic quadriceps femoris muscle defect. *Orthopedics* 33: 511, 2010.

37. **Merritt EK, Cannon MV, Hammers DW, Le LN, Gokhale R, Sarathy A, Song TJ, Tierney MT, Suggs LJ, Walters TJ, Farrar RP.** Repair of traumatic skeletal muscle injury with bone-marrow-derived mesenchymal stem cells seeded on extracellular matrix. *Tissue Eng Part A* 16: 2871–2881, 2010.

38. **Messina LM, Carlson BM.** Rapid and complete recovery of responsiveness to adenosine and norepinephrine by regenerating arterioles of the tibialis anterior muscle of the hamster after in situ autografting. *Circ Res* 68: 1600–1609, 1991.

39. **Meyer GA, Lieber RL.** Skeletal muscle fibrosis develops in response to desmin deletion. *Am J Physiol Cell Physiol* 302: C1609–C1620, 2012.

40. **Murphy MM, Lawson JA, Mathew SJ, Hutcheson DA, Kardon G.** Satellite cells, connective tissue fibroblasts and their interactions are crucial for muscle regeneration. *Development* 138: 3625–3637, 2011.

41. **Natsu K, Ochi M, Mochizuki Y, Hachisuka H, Yanada S, Yasunaga Y.** Allogeneic bone marrow-derived mesenchymal stromal cells promote the regeneration of injured skeletal muscle without differentiation into myofibers. *Tissue Eng* 10: 1093–1112, 2004.

42. **Nieminen H, Kuokkanen H, Tukiainen E, Asko-Seljavaara S.** Free flap reconstructions of tibial fractures complicated after internal fixation. *J Trauma* 38: 660–664, 1995.

43. **Patzkowski JC, Blanck RV, Owens JG, Wilken JM, Kirk KL, Wenke JC, Hsu JR; Skeletal Trauma Research Consortium.** Comparative effect of orthosis design on functional performance. *J Bone Joint Surg Am* 94: 507–515, 2012.

44. **Plant DR, Colarossi FE, Lynch GS.** Notexin causes greater myotoxic damage and slower functional repair in mouse skeletal muscles than bupivacaine. *Muscle Nerve* 34: 577–585, 2006.

45. **Rathbone CR, Wenke JC, Warren GL, Armstrong RB.** Importance of satellite cells in the strength recovery after eccentric contraction-induced muscle injury. *Am J Physiol Regul Integr Comp Physiol* 285: R1490–R1495, 2003.

46. **Rosenblatt JD, Parry DJ.** Gamma irradiation prevents compensatory hypertrophy of overloaded mouse extensor digitorum longus muscle. *J Appl Physiol* 73: 2538–2543, 1992.

47. **Rossi CA, Flaibani M, Blaauw B, Pozzobon M, Figallo E, Reggiani C, Vitiello L, Elvassore N, De Coppi P.** In vivo tissue engineering of functional skeletal muscle by freshly isolated satellite cells embedded in a photopolymerizable hydrogel. *FASEB J* 25: 2296–2304, 2011.

48. **Saclier M, Yacoub-Youssef H, Mackey AL, Arnold L, Ardjoune H, Magnan M, Sailhan F, Chelly J, Pavlath GK, Mounier R, Kjaer M, Chazaud B.** Differentially activated macrophages orchestrate myogenic precursor cell fate during human skeletal muscle regeneration. *Stem Cells* 31: 384–396, 2013.

49. **Salafsky B.** Functional studies of reenerated muscles from normal and dystrophic mice. *Nature* 229: 270–272, 1971.

50. **Sambasivan R, Yao R, Kissenpfennig A, Van Wittenberghe L, Paldi A, Gayraud-Morel B, Guenou H, Malissen B, Tajbakhsh S, Galy A.** Pax7-expressing satellite cells are indispensable for adult skeletal muscle regeneration. *Development* 138: 3647–3656, 2011.

51. **Sen MK, Miclau T.** Autologous iliac crest bone graft: should it still be the gold standard for treating nonunions? *Injury* 38, Suppl 1: S75–80, 2007.

52. **Smith CA, Stauber F, Waters C, Alway SE, Stauber WT.** Transforming growth factor-beta following skeletal muscle strain injury in rats. *J Appl Physiol* 102: 755–761, 2007.

53. **Stauber WT, Knack KK, Miller GR, Grimmett JG.** Fibrosis and intercellular collagen connections from four weeks of muscle strains. *Muscle Nerve* 19: 423–430, 1996.

54. **Stern MM, Myers RL, Hammam N, Stern KA, Eberli D, Kritchevsky SB, Soker S, Van Dyke M.** The influence of extracellular matrix derived from skeletal muscle tissue on the proliferation and differentiation of myogenic progenitor cells ex vivo. *Biomaterials* 30: 2393–2399, 2009.

55. **Studitsky AN.** Free auto- and homografts of muscle tissue in experiments on animals. *Ann NY Acad Sci* 120: 789–801, 1964.

56. **Sun G, Haginoya K, Wu Y, Chiba Y, Nakanishi T, Onuma A, Sato Y, Takigawa M, Iinuma K, Tsuchiya S.** Connective tissue growth factor is overexpressed in muscles of human muscular dystrophy. *J Neurol Sci* 267: 48–56, 2008.

57. **Suzuki K, Murtuza B, Heslop L, Morgan JE, Smolenski RT, Suzuki N, Partridge TA, Yacoub MH.** Single fibers of skeletal muscle as a novel graft for cell transplantation to the heart. *J Thorac Cardiovasc Surg* 123: 984–992, 2002.

58. **Tateyama M, Fujihara K, Misu T, Itoyama Y.** CCR7+ myeloid dendritic cells together with CCR7+ T cells and CCR7+ macrophages invade CCL19+ nonnecrotic muscle fibers in inclusion body myositis. *J Neurol Sci* 279: 47–52, 2009.

59. **Tatsumi R, Anderson JE, Nevoret CJ, Halevy O, Allen RE.** HGF/SF is present in normal adult skeletal muscle and is capable of activating satellite cells. *Dev Biol* 194: 114–128, 1998.

60. **Tidball JG.** Inflammatory processes in muscle injury and repair. *Am J Physiol Regul Integr Comp Physiol* 288: R345–R353, 2005.

61. **Tsai SW, Chen CJ, Chen HL, Chen CM, Chang YY.** Effects of treadmill running on rat gastrocnemius function following botulinum toxin A injection. *J Orthop Res* 30: 319–324, 2012.

62. **Turner NJ, Badylak JS, Weber DJ, Badylak SF.** Biologic scaffold remodeling in a dog model of complex musculoskeletal injury. *J Surg Res* 176: 490–502, 2012.

63. **Turner NJ, Yates AJ Jr, Weber DJ, Qureshi IR, Stolz DB, Gilbert TW, Badylak SF.** Xenogeneic extracellular matrix as an inductive scaffold for regeneration of a functioning musculotendinous junction. *Tissue Eng Part A* 16: 3309–3317, 2010.

64. **Valentin JE, Stewart-Akers AM, Gilbert TW, Badylak SF.** Macrophage participation in the degradation and remodeling of extracellular matrix scaffolds. *Tissue Eng Part A* 15: 1687–1694, 2009.

65. **Valentin JE, Turner NJ, Gilbert TW, Badylak SF.** Functional skeletal muscle formation with a biologic scaffold. *Biomaterials* 31: 7475–7484, 2010.

66. **Van Handel PJ, Watson P, Troup J, Plyley M.** Effects of treadmill running on oxidative capacity of regenerated skeletal muscle. *Int J Sports Med* 2: 92–96, 1981.

67. **Warren GL, Hulderman T, Mishra D, Gao X, Millecchia L, O'Farrell L, Kuziel WA, Simeonova PP.** Chemokine receptor CCR2 involvement in skeletal muscle regeneration. *FASEB J* 19: 413–415, 2005.

68. **White TP, Villanacci JF, Morales PG, Segal SS, Essig DA.** Exercise-induced adaptations of rat soleus muscle grafts. *J Appl Physiol* 56: 1325–1334, 1984.

69. **Willett NJ, Li MT, Uhrig BA, Boerckel JD, Huebsch N, Lundgren TL, Warren GL, Guldberg RE.** Attenuated human bone morphogenetic protein-2-mediated bone regeneration in a rat model of composite bone and muscle injury. *Tissue Eng Part C Methods* 19: 316–325, 2013.

70. **Wolf MT, Daly KA, Reing JE, Badylak SF.** Biologic scaffold composed of skeletal muscle extracellular matrix. *Biomaterials* 33: 2916–2925, 2012.

71. **Wu X, Corona BT, Chen X, Walters TJ.** A standardized rat model of volumetric muscle loss injury for the development of tissue engineering therapies. *Biores Open Access* 1: 280–290, 2012.